ORIGINAL PAPER

Structural and mechanical properties of fibrous poly (caprolactone)/gelatin nanocomposite incorporated with cellulose nanofibers

Zahra Moazzami Goudarzi[1] · Tayebeh Behzad[1] · Laleh Ghasemi-Mobarakeh[2] · Mahshid Kharaziha[3] · Mohammad Saied Enayati[1,4]

Abstract

To proceed with the electrospun poly (caprolactone) (PCL)/gelatin (Gel) combinations, the current research was aimed to explore the incorporation of cellulose nanofibers (CNF) into the PCL/Gel blends for the first time. Accordingly, various amounts of CNF were added to different ratios of PCL/Gel, and the corresponding electrospun nanocomposites were examined. Observing morphology via scanning electron microscopy proved, unexpectedly, increasing fibers diameter upon CNF addition into PCL/Gel blends. Mechanical analysis in tensile mode revealed more brittle electrospun PCL/Gel when more Gel was included into the blend due to higher Young's modulus and lower ultimate tensile strength and strain at break. Addition of various contents of CNF led to strain reduction while displayed a summit-like curve for UTS and modulus, where registered maximum values at 2 wt% CNF for all PCL/Gel/CNF. Among the electrospun nanocomposites the highest UTS (3.24 ± 0.22 MPa) belonged to sample including 70 wt% PCL, 30 wt% Gel, and 2 wt% CNF (P70/2CNF), while P30/2CNF recorded maximum modulus (93.89 ± 10.44 MPa). The wide-angle X-ray scattering confirmed increase in PCL crystallinity upon CNF incorporation Furthermore, the presence of PCL, Gel, and CNF in electrospun composites was confirmed with Fourier transform infrared spectroscopy. Degradability of electrospun nanocomposites was carried out in PBS solution, which showed that CNF addition reduced degradation rate of PCL/Gel blends.

Keywords Poly (caprolactone) · Gelatin · Cellulose nanofibers · Electrospun nanocomposite

---

✉ Tayebeh Behzad
tbehzad@cc.iut.ac.ir

Extended author information available on the last page of the article

🙋 Springer

Introduction

Biopolymers, either synthetic or naturally occurring, have gained a tremendous attention in recent decades in various research fields such as biomedical engineering (e.g., tissue engineering, drug delivery, etc.), membrane science, and packaging to name just a few [1–6]. Biomimic of natural tissues as well as environmental concerns is the main contribution toward the use of such biodegradable and biocompatible polymers. Considering the biomedical applications, both synthetic and natural biopolymers have their own merits and demerits. For example, the natural ones, e.g., gelatin, chitosan, alginate, possess active chemical surface (hydrophilic nature) which mimics the natural tissues; however, they suffer from inadequate mechanical properties [7–9]. Oppositely, their synthetic counterparts, e.g., PCL [10], lack the favorable active surface; however, they have better mechanical characteristics. Although a combination of both can, to some extent, overcome the mentioned limitations, biomedical applications, especially tissue engineering, require stiffer constructs which could tolerate the mechanical shocks during regeneration of damaged tissues. In this regard, nanomaterials have been successfully utilized to address these obstacles due to the beneficial characteristics such as large surface area to volume ratio [11, 12]. Hence, the innovative combinations of biopolymer and nanoscaled materials can simulate the natural tissues from chemical, mechanical, and biological view points, and consequently, introduce the most promising materials for biomedical applications [13, 14].

Good solubility, low melting temperature, and excellent processability of PCL make it as great potential for biomedicine applications [15]. Furthermore, its low rate of degradation meets the requirements for fabrication of implants, drug delivery devices, scaffolds, and sutures in which longer degradability is expected [16]. However, the hydrophobic nature of PCL has drawn scientists' attention to overcome such drawback through blending with natural polymers and also incorporation of nanofillers [17–21]. Gelatin, hydrolyzed form of collagen, is one the most ideal native biopolymers which can be blended with PCL in order to improve its lack of hydrophilicity [22, 23].

Among the important features of intended structures (scaffolds) for tissue engineering applications, porosity plays a vital role [24]. Various approaches have been applied for fabrication of porous architectures including electrospinning [25–27], phase separation [28, 29], freeze drying [30, 31], and supercritical fluid [32–34], while the electrospinning has gather a great deal of interest mainly because of simplicity, low cost, scalable, and well control on morphology of the fibers [35]. In addition, it has been proved that electrospun fibers can boost mechanical performance of fabric-reinforced composites. In one contribution, Razavi et al. [36] studied the effect of poly (acrylonitril) electrospun nanofibers incorporation into epoxy-based adhesives. More recently, this group explored the addition of Al_2O_3-reinforced electrospun nanofibers into carbon/epoxy composites [37]. Both researches showed increase in fracture energy of composites due to the nanofiber incorporation, i.e., nanofibers toughened the composites.

In recent years, several reports have been presented on electrospun PCL/Gel fibers [38–43]. In a pioneering attempt, conducted by Zhang et al. [44], PCL/Gel mixture noticeably improved the cell proliferation and infiltration compared to the pure PCL. Furthermore, Densi et al. [45], Gautam et al. [46], and Ren et al. [42] studied electrospun PCL/Gel for tissue engineering applications with the focus on using less harmful solvents. Rajers et al. [47] also electrospun nanofibrous scaffolds composed of calcium phosphate-modified PCL and Gel for bone tissue engineering. There is also a bulk of researches on the incorporation of nanomaterials into the electrospun biopolymers with the aim of promoting mechanical and biological properties. Meanwhile, there has been growing interest in developing nanocomposites including nanoscaled cellulose materials such as cellulose nanowhiskers [48], cellulose nanofibers [49, 50], and cellulose nanocrystals [51, 52], thanks to their particular features, i.e., large aspect ratio, high Young's modulus, biocompatibility, biodegradability, low toxicity, cheap, and renewable resources [53]. Recently, Enayati et al. exploited such advantages to develop PVA/nanohydroxy apatite (nHAp) electrospun mats reinforced with cellulose nanofibers for bone tissue engineering with enhanced cell growth properties [54]. In addition, PCL- or Gel-reinforced electrospun fibers using cellulosic materials were also prepared by others [55, 56]; however, up to now, to the best of our knowledge, there is no report on preparation of PCL/Gel nanocomposites incorporated with cellulose nanomaterials. Therefore, in this contribution, to go beyond the present state of the art in combination of the synthetic and natural biopolymers with naturally originated nanomaterials, for the first time, for the fabrication and characterization of fibrous nanocomposites containing PCL/Gel, cellulose nanofibers are introduced. In this content, it is mainly concentrated on preparation of electrospun PCL/Gel (as matrix)/cellulose nanofibers (as fillers) in various ratios of the compositions. Moreover, the structure and properties of electrospun mats were systematically characterized applying diverse analyses. Finally, the in vitro degradation of the mats was studied in PBS solution.

Experimental

Materials

Poly (Caprolactone) (PCL), molecular weight of 80,000 g/mol and Gelatin type A from porcine skin, were supplied by Sigma-Aldrich. Cellulose nanofibers were extracted from wheat straw by chemo-mechanical procedure in laboratory scale as described earlier [49]. The average diameter of nanofibers was obtained to be around 30 nm. Glacial acetic acid (AA), pure formic acid (FA), and ethanol (98%) were all supplied from Merck. Deionized water was used throughout the work.

Procedures

Preparation of PCL/Gel solutions

A solvent system including AA and FA, in a ratio of 3(AA):1(FA), was used for dissolving PCL/Gel blends [45]. Three different polymer weight combinations, i.e., 70(PCL)/30(Gel), 50(PCL)/50(Gel), and 30(PCL)/70(Gel) were chosen and coded as P70, P50, and P30, respectively. In addition, different polymer solutions containing PCL and Gel with concentrations of 9, 10, 11, and 12 wt% were prepared.

Preparation of PCL/Gel/CNF suspensions

Firstly, aqueous CNF suspension was solvent-exchanged from water to the solvent system. For this aim, water content of CNF was totally discharged by pure ethanol; subsequently, ethanol was replaced by binary solvent system. Resulted suspensions of each stage were exposed to both ultrasonic (400 W, for 10 min) and stirring (20 min), respectively, to ensure solvent exchange [51]. Afterward, the certain amounts (1, 2, 3, and 6 wt% respect to the polymer) of CNF suspension were added to 10 wt% solution of PCL/Gel combinations (P70, P50, and P30). This 10 wt% solution was opted according to the morphological characterization of electrospun fibers which will be explained later.

Electrospinning process

The electrospinning equipment (MEDIFUSION MS-2200, Daiwha, South Korea) was operated in horizontal mode. It is consisted of a single syringe pump (TERUMO ATC-527, Japan), steel plate collector, and a high-voltage generator (EMERSUN), connected with positive terminal to a stainless steel needle and grounded to the collector. For electrospinning of PCL/Gel solutions, collection distance (*d*) selected to be 13 cm. Applied voltage was varied between 11 and 14 kV, flow rates of solution were 0.1 and 0.2 mL/h, and a needle with 0.23 mm inner diameter was used. The electrospun mats were stored at room temperature until further use.

Characterizations

The electrical conductivity and viscosity measurements

Brookfield DV-II Viscometer (USA) and JENWA 3540 conductivity meter were employed to measure the conductivity and viscosity of suspensions. Viscosity was measured at the rotational speed of 6 rpm and temperature of 22 °C.

Scanning electron microscopy (SEM)

Qualitative and quantitative morphological analysis of electrospun fibers was performed using the scanning electron microscope (SEM Philips XL3, Netherland) instrument at accelerating voltage of 12 kV. Prior to observations, samples were coated with a layer of gold. The mean fiber diameter for particular sample was estimated from 200 measurements on a particular SEM image. Diameter distributions were analyzed using Gaussian function approximation (Origin software).

Fourier transform infrared spectroscopy (FTIR)

To chemically analyze the electrospun samples, the IR spectra were recorded in ATR-FTIR mode using RAYLEIGH WQF510A spectrophotometer (China). The samples were scanned in the range of 400–4000 cm^{-1}.

Wide-angle X-ray scattering (WAXS)

To explore the effects of electrospinning and filler addition on the supermolecular structure of PCL/Gel and its nanocomposites, WAXS measurements were carried out using ASENWARE AW-XDM300 diffractometer (China) (CuK_α radiation, $\lambda = 1.5418$ Å). For all samples, "coupled theta—2θ" scans were performed in the range of 10°–60° with the steps of 0.04°/s, the beam power of 1600 W, and time of data acquisition of 1 s/step.

In addition, crystallinity degree (χ_c) was calculated from the ratio of the sum of areas under the crystalline peaks (A_c) to area of all peaks (Eq. 1) in the investigated range of angles, where A_m is the area under amorphous halo [48].

$$\chi_c = A_c / (A_c + A_m) \tag{1}$$

Differential scanning calorimetry (DSC)

Thermal behavior of the electropsun fibers were investigated using differential scanning calorimeter (BAR, DSC 302, Germany). Samples (about 5 mg) were scanned during heating stage from 27 to 78 °C at the rate of 10 °C/min.

Tensile test

The mechanical performance of electrospun mats were analyzed by uniaxial extension (Zwick Universal Testing Machine-144660, Germany) with a 20 N load cell under a cross-head speed of 10 mm/min [57]. The samples with an adequate thickness (around 100 μm) were cut into 10×30 mm^2 rectangles (a typical picture of test specimen is seen in Fig. 1) and placed in the grips with a gauge length of 20 mm. Five samples were tested for each type of electrospun mat. The thickness was averaged from seven measurements performed by the digital micrometer. The
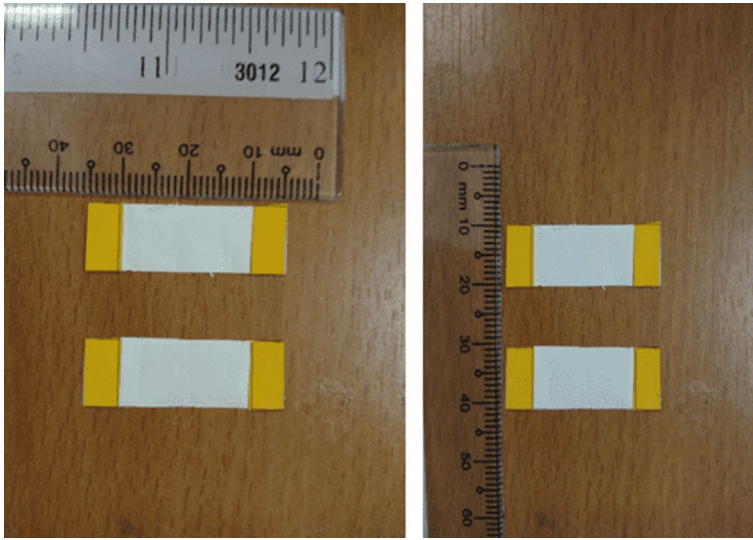
Fig. 1 Typical picture of tensile test specimen

ultimate tensile stress (UTS), elongation at break (EB), and tensile modulus (E) were determined from stress–strain plots.

In vitro biodegradation

Biodegradability of the electrospun nanocomposites was studied according to ASTM F 1635. The samples were incubated in phosphate-buffered saline (PBS) solution for various intervals, i.e., 1, 2, 3, 5, 7, 14, 21, 28, and 60 days. The initial weight (W_0) and weight at time t (W_t) were recorded for each sample, and the degradation index (D) was calculated using Eq. 2 [54].

$$D = \left(W_0 - W_t\right)/W_0 \tag{2}$$

Statistical method

The quantitative data were presented as the mean $\pm$ SD ($n = 3$) and analyzed using Student's t test or one-way ANOVA by SPSS software (version 16.0). The values of $P < 0.05$ were considered statistically significant.

Results and discussion

Electrical conductivity and viscosity of samples

Table 1 displays the impact of polymer ratio changes (PCL/Gel) on both viscosity and electrical conductivity of the solutions, which are well known as efficient parameters on electrospinning. The total concentration of PCL/Gel maintained at

Table 1 Changes in viscosity and electrical conductivity of the solutions

Sample	PCl wt%	Gel wt%	Viscosity (cP)	Conductivity (µS)
P70	70	30	384.9	221
P50	50	50	338.9	370
P30	30	70	248.9	558

10 wt%. It can be seen from this table that increase in Gel content acts differently on viscosity and conductivity of solutions, as the former reduced while the latter rose. In terms of viscosity, this observation is in agreement with the reports of Denis et al. [45] for PCL/Gel that they explained, irrespective of solvent, viscosity was reduced by increasing Gel content. For AA/FA (90:10) solvent system, this group reported 80 µS/cm electrical conductivity for a mixture including 25% Gel. The increase in conductivity can be attributed to the higher polar native of Gel compared to PCL due to the probable ionization of amino and carboxyl groups within chemical structure of gelatin [45].

Considering the CNF (2 wt%) loaded solutions (Table 2), conductivity shows increasing manner compared to none-loaded PCL/Gel which can be explained from two points of view. On the one hand, it has been reported that conductivity directly varies with crystallinity [58]. Therefore, it is anticipated that by incorporation of crystalline CNF into the PCL/Gel solution, the conductivity will be grown. On the other hand, increase in conductivity after CNF addition can be attributable to the negative charges from sulfate ester groups on the surface of CNFs, which grafted from sulfuric acid during bleaching stage in isolation of CNF [49]. The effect of CNF incorporation on viscosity undergoes a different manner, as for P30 (containing 70 wt% of Gel) this parameter was increased (from 248.9 cP to 296.9 cP), while for the two others, it was reduced approximately 9.1% (for P70) and 7.9% (for P50). The higher interactions between CNF and Gel in P30 compositions induce more restrictions on polymeric chains and could be the possible reason for viscosity increase. For all data presented in Tables 1 and 2, the changes were statistically significant ($P < 0.05$).

Morphology of electrospun mats

Besides the electrospinning of three different blends of PCL/Gel, pure PCL and Gel were also electrospun. The SEM images of the nonwoven mats are presented

Table 2 Effect of CNF addition on viscosity and electrical conductivity of the PCl/Gel blends

Sample	PCl wt%	Gel wt%	Viscosity (cP)	Conductivity (µS)
P70+ 2%CNF	70	30	349.9	226
P50+ 2%CNF	50	50	311.9	400
P30+ 2%CNF	30	70	296.9	620

PCL

Mean = 127.63
Std.Dev. = 25.87
N = 200

Gel

Mean = 299.73
Std.Dev. = 39.21
N = 200

P70

Mean = 95.88
Std.Dev. = 11.18
N = 200

P50

Mean = 177.89
Std.Dev. = 38.62
N = 200

P30

Mean = 250.94
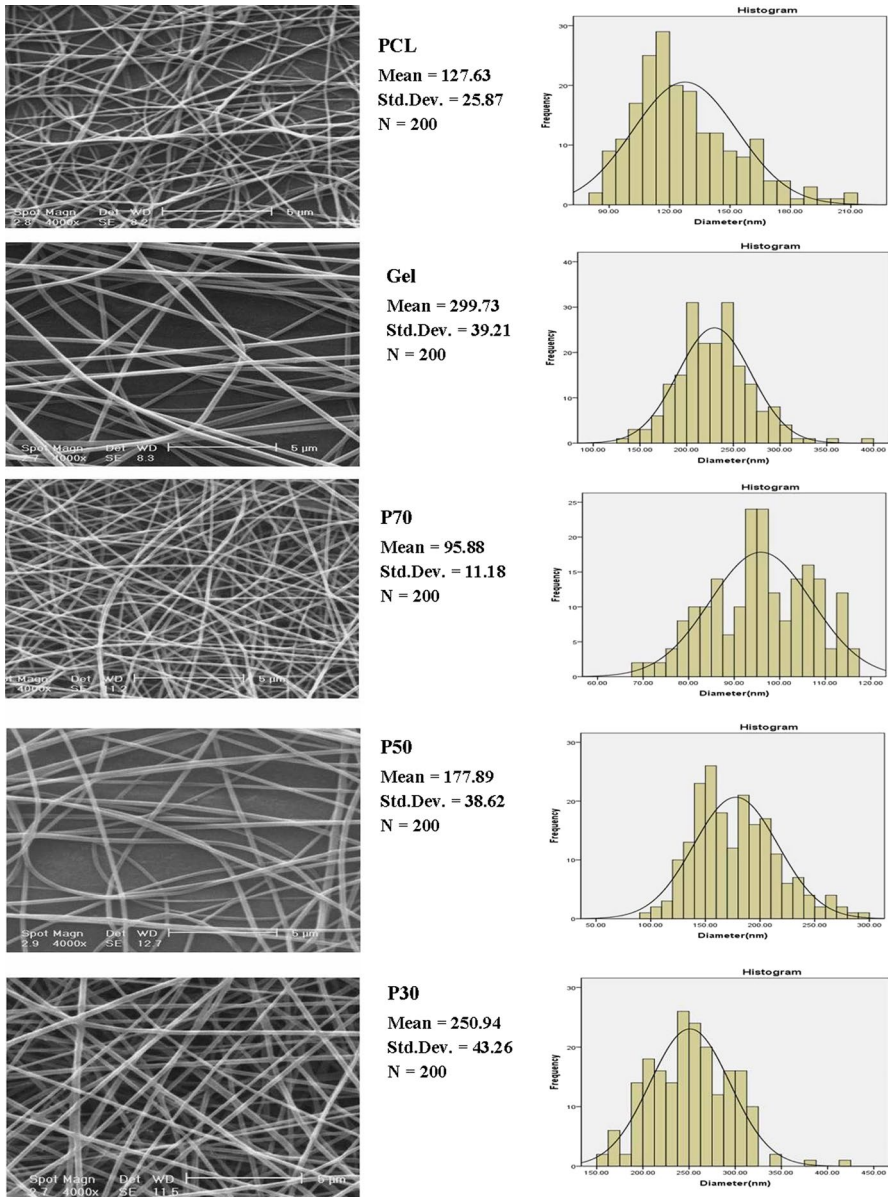Std.Dev. = 43.26
N = 200

Fig. 2 SEM images of electrpspun PCL, Gel, and their blends in different ratios

in Fig. 2. As it can be observed, compared to pure PCL, pure Gel nanofibers are more uniform in fiber diameter, while possess higher diameter. Upon 30 wt% addition of Gel to PCL (P70), the uniformity of fibers, in comparison with pure PCL, was improved, and the mean fiber diameter was reduced dramatically, from 127.63 ± 25.88 nm to 95.88 ± 11.18 nm. Such reduction in diameter is interpretable

via noticeable variations in viscosity and conductivity by Gel addition (Table 1). It has been widely reported that decrease in viscosity and increase in conductivity should lead to the fiber diameter reduction [49]. Upon the higher loading of the Gel, although the more uniform fibers were achieved, the fiber diameter trend diversely altered, i.e., an increase in fiber diameter was observed. These finding completely agree with the Denis et al. observations for electrospun fibers obtained from a PCL/Gel in AA (90): FA (10) solutions [45]. It is believed that such quite unexpected increase in fiber diameter of PCL/Gel fibers with increasing Gel content was most probably arisen from the presence of emulsion, which can be highlighted at higher Gel content [45].

Subsequently, various amounts of CNF (1, 2, 3, and 6 wt%) were added to the PCL/Gel blends and electropsun. According to the mechanical investigations, described in the next part, for all PCL/Gel compositions, the optimized properties were recorded at 2 wt% of CNF. Consequently, samples with other CNF contents were excluded from morphological assessments. The SEM images of PCL/Gel electrospun nanofibers at 2 wt% of CNF are presented in Fig. 3. In addition, the associated mean fiber diameters are listed in Table 3. According to this table, it is indicated that CNF incorporation ended to fiber diameter increase for all PCL/Gel compositions where the statistical significance belongs to the 2 wt%-P70 sample ($P < 0.05$), while the mean fiber diameter of P50 and P30 were not statistically significant ($P > 0.05$), in comparison with their pure counterparts. Taking into account the data presented in Table 2, CNF addition caused reduction in the viscosity (except P30) and increase in the conductivity, and hence a decreasing trend in fiber diameter should be expected. However, practically, the fiber diameter shows an increasing manner. Such behavior, repeatedly as described earlier for PCL/Gel blends, might be due to the emulsion existence which might be intensified in the presence of CNF's [45].

Mechanical properties

Due to the importance of mechanical properties of fibrous materials in various applications, e.g., tissue engineering, the electrospun samples were mechanically examined via tensile test. Accordingly, pure polymeric electrospun mats, i.e., PCL and Gel, were stretched as their typical stress–strain curves are shown in Fig. 4. It is evident that PCL behaves like a soft material with low Young's modulus and relatively high strain, while Gel shows brittle characteristic, i.e., high stiffness but low elongation at break, which is in coincidence with former reports [44].

For PCL/Gel blends, the tensile properties were affected by the weight ratio of the neat polymers in the mixture, for instance at the higher PCL content, the electrospun nonwoven possesses lower stiffness, but higher ultimate tensile stress and elongation at break (Fig. 5). On the contrary, Gel contribution is toward stiffening the blends as, for P30 (including 70% Gel), the stress–strain performance more resembles the neat Gel. The similar manner was observed by Ghasemi-Mobarakeh et al. in blending PCL and Gel, as platforms for nerve tissue engineering [38].
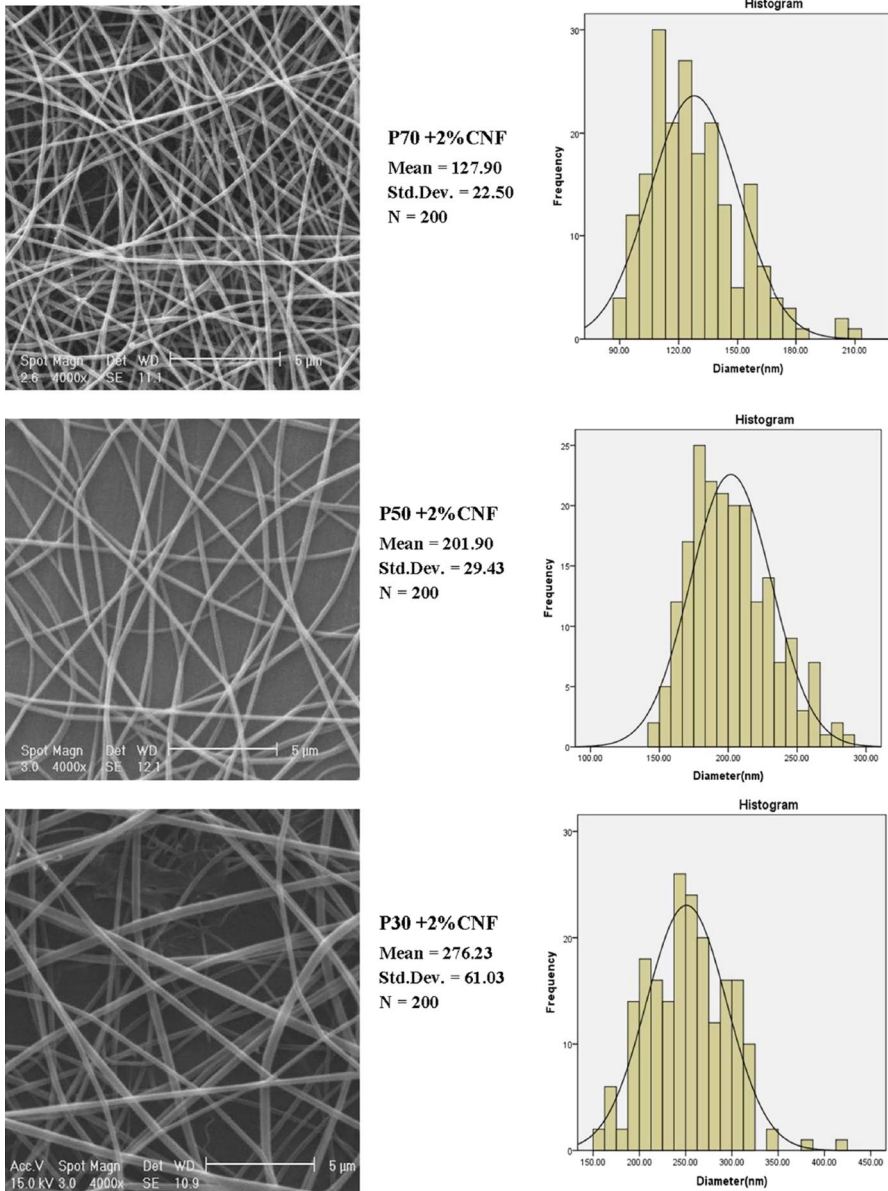
P70 +2%CNF
Mean = 127.90
Std.Dev. = 22.50
N = 200

P50 +2%CNF
Mean = 201.90
Std.Dev. = 29.43
N = 200

P30 +2%CNF
Mean = 276.23
Std.Dev. = 61.03
N = 200

Fig. 3 SEM images of P70, P50, and P30 incorporated with 2 wt% CNF

To explore the influence of CNF content on tensile properties of PCL/Gel nonwoven webs, 1, 2, 3, and 6 wt% of CNF were incorporated into P70, P50, and P30. The averaged mechanical properties, i.e., Young's modulus (E), ultimate tensile strength (UTS), and elongation at break (strain) of related fibrous samples, i.e., nanocomposites, PCL, Gel, and PCL/Gel, are presented in Table 4. The statistical analysis

Table 3 Effect of CNF addition on mean fiber diameter

Sample	PCl wt%	Gel wt%	Mean fiber diameter (nm)
P70	70	30	95.88 ± 11.18
P70+ 2%CNF	70	30	127.90 ± 22.50
P50	50	50	177.89 ± 38.62
P50+ 2%CNF	50	50	201.90 ± 29.43
P30	30	70	250.94 ± 43.27
P30+ 2%CNF	30	70	276.23 ± 61.03
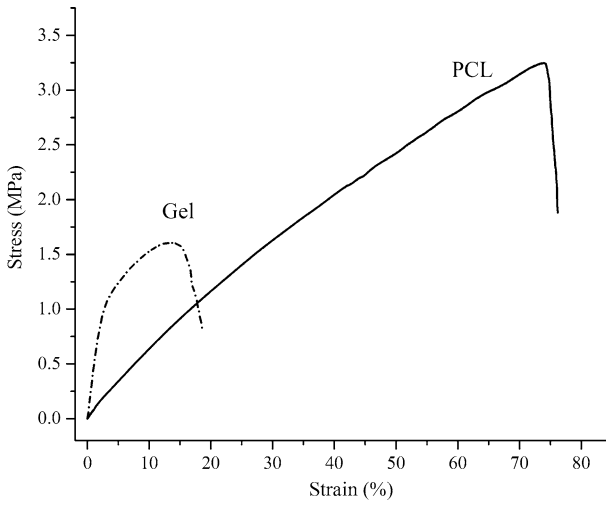
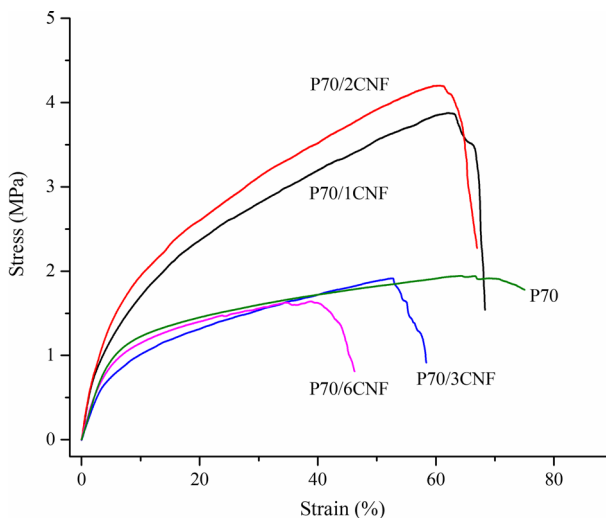**Fig. 4** Typical stress–strain curves of electrospun PCL and Gel
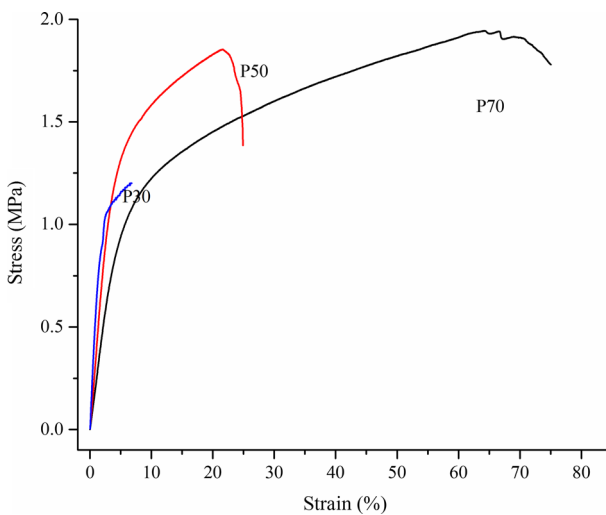
Fig. 5 Typical stress–strain curves of electrospun PCL/Gel blends

Table 4 Tensile properties of electrospun PCL, Gel, PCL/Gel, and PCL/Gel/CNF

Sample	PCL (wt%)	Gel (wt%)	CNF (wt%)	UTS (MPa)	E (MPa)	Strain (%)
PCL	100	0	0	2.40±0.15	6.14±0.54	71.03±4.16
Gel	0	100	0	1.80±0.13	47.49±2.34	13.10±1.69
P70	70	30	0	2.66±0.24	22.52±1.76	68.73±24.55
P70/1CNF	70	30	1	2.40±0.4	21.46±2.3	68.67±13.08
P70/2CNF	70	30	2	3.24±0.22	25.75±1.71	61.46±4.5
P70/3CNF	70	30	3	2.07±0.19	22.23±3.43	50.25±6.09
P70/6CNF	70	30	6	1.54±0.25	19.88±0.83	38.48±11.17
P50	50	50	0	1.69±0.25	38.16±5.22	22.02±9.27
P50/1CNF	50	50	1	1.51±0.16	37.60±4.86	21.71±4.58
P50/2CNF	50	50	2	2.51±0.15	53.06±5.3	30.29±5.99
P50/3CNF	50	50	3	1.79±0.15	42.13±8.76	20.53±3.94
P50/6CNF	50	50	6	1.41±0.18	36.76±3.5	15.30±7.15
P30	30	70	0	1.29±0.3	66.83±10.37	6.80±2.31
P30/1CNF	30	70	1	1.54±0.2	78.17±7.37	5.53±1.83
P30/2CNF	30	70	2	2.06±0.52	93.89±10.4	4.85±0.85
P30/3CNF	30	70	3	1.32±0.3	73.38±12.22	4.12±0.61
P30/6CNF	30	70	6	1.77±0.10	57.85±5.94	8.44±1.64

showed significant changes in mechanical properties ($P < 0.05$). In a general view, it can be noticed that CNF addition was led to the gradual reduction in strain for PCL/Gel mats (excluding P30/6CNF), which is a ubiquitous phenomenon upon inclusion of high stiff phases into the polymers [59]. In a research conducted by Enayati et al., it was demonstrated that incorporation of nHAp and CNF into PVA nanofibers

Fig. 6 Typical stress–strain curves of electrospun P70/CNF nanocomposites

resulted in dramatic decrease in elongation at break in comparison with neat PVA nanofibers [49]. In a different trend, the CNF loading recorded a maximum at 2 wt% for UTS and Young's modulus as the both properties were increased after 1 and 2 wt% CNF addition; however, the further CNF resulted in reduction in these properties (Fig. 6), which might be attributed to the defects inserted by rigid CNF nanomaterials or agglomeration of CNF in higher contents. The increase in mechanical performance of nanocomposites at low levels of CNF could be due to better dispersion within the polymeric matrix, thus resulting in more interaction between filler and matrix phases and better stress transition. The higher CNF content is probably susceptible to agglomeration formation, due to possible hydrogen bonding among CNF molecules. More deeply considering the obtained results, it is elucidated that, for example, at 2 wt% of CNF, addition of more Gel has been resulted in higher increase in UTS and modulus, compared to non-loaded PCL/Gel. In the case of UTS, samples of P70/2CNF, P50/2CNF, and P30/2CNF showed 21.8%, 48.52%, and 59.69% increase compared with P70, P50, and P30, respectively. Similarly, Young's modulus improvement was calculated to be 14.3%, 39.04%, and 40.5% for P70/2CNF, P50/2CNF, and P30/2CNF, respectively. High affinity between CNF and Gel, through hydrogen bonding as described in Fig. 7, might be the explanation for such reinforcement behavior. In fact, higher Gel content would boost the physical cross-linking, in the form of hydrogen bond interactions, among Gel and CNF within the nanocomposite.

From another perspective, as reported above, incorporating both Gel and CNF led to reduction in PCL elongation, i.e., either fibrous PCL blends or nanocomposites become more brittle than pure PCL fibers. Fracture surface of electrospun fibers by electron microscopy was observed to compare the fracture mechanism; however, due to the small fibers' thickness, at high magnifications, they were easily bent and the surface fracture observation was impossible, as earlier reported by Enayati et al. [50].
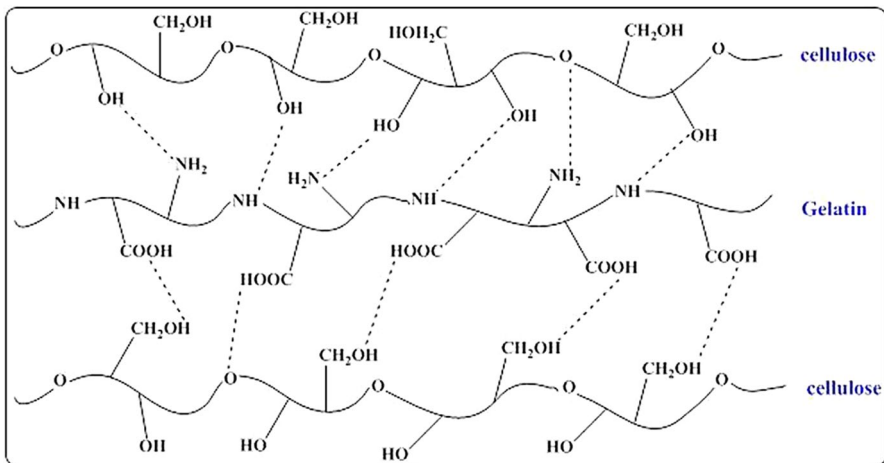

Fig. 7 Hydrogen bond interactions between CNF and Gel

It can be concluded that for all PCL/Gel blends, the CNF optimum level is 2 wt%, in which UTS and modulus were maximized (Fig. 6). Consequently, further analyses, i.e., SEM, FTIR, and XRD, were carried out on samples including this CNF quantity.

Tissue engineering is one the potential applications for electrospun porous nonwovens (scaffold), in which the aim is to regenerate a damaged body tissue. From the mechanical point of view, the scaffold has to approximate the mechanical properties of host tissues, in order to withstand the imposed mechanical shocks within the tissue regeneration. Among the mechanical properties, the elastic modulus plays a vital role which is different for various natural tissues. According to the reported values for moduli of different body tissues, the various combinations of PCL/Gel/CNF (Table 4) fabricated during this study could cover the required stiffness for scaffolds in tissue engineering of nerve, saphenous vein, arterial wall, cartilage, heart, tendon/ligament, skin, and soft bone [60].

Wide-angle X-ray scattering (WAXS)

It has been widely reported, as we also observed in this study, that PCL, as a semicrystalline polymer, has strong crystalline peaks positioned at Bragg angles of $2\theta = 21.3°$ and 23.6° which can be assigned to crystalline planes of (1 0 0) and (2 0 0), respectively (Fig. 8) [61]. In Fig. 8, the WAXS patters of granular and electrospun PCL are shown through which crystallinity of samples was estimated to be 59.42% and 55.09%, respectively. The reduction in crystallinity of semicrystalline polymers after electrospinning can be due to extremely short time of the solvent evaporation during the process resulting in crystallization prevention at the early
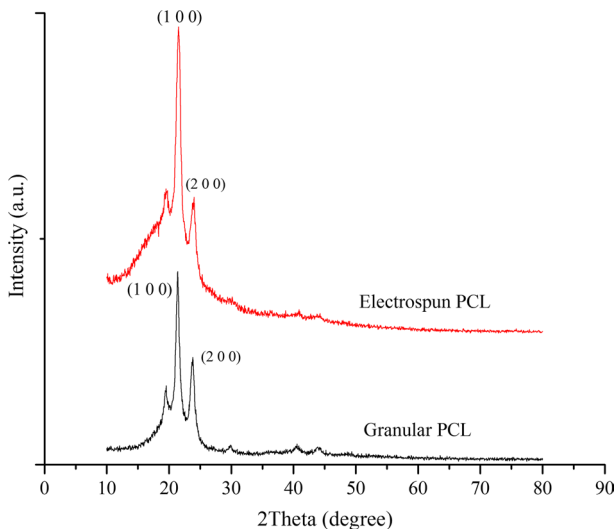

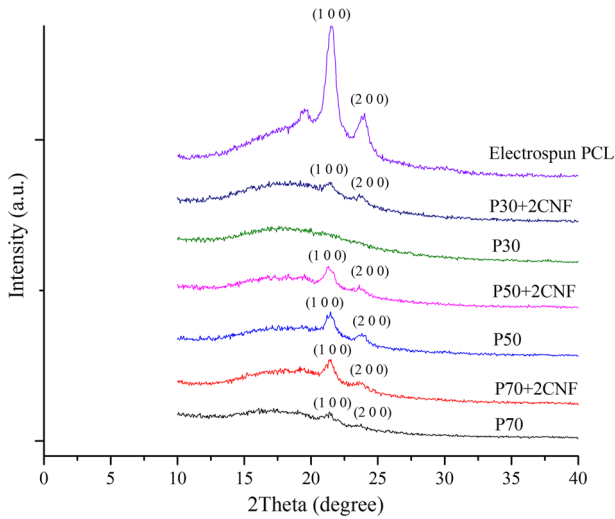**Fig. 8** WAXS profiles of granular and electrospun PCL

Fig. 9 WAXS profiles of electrospun PCL, PCL/Gel blends, and their nanocomposites

Table 5 Crystallinity of electrospun PCL/Gel blends and their nanocomposites

Sample	PCl wt%	Gel wt%	Crystallinity (%)
Granular PCL	100	0	59.42
Electrospun PCL	100	0	55.09
P70	70	30	50.11
P70+ 2%CNF	70	30	56.82
P50	50	50	31.80
P50+ 2%CNF	50	50	40.7
P30	30	70	21.92
P30+ 2%CNF	30	70	24.49

stage [49, 62]. Inversely, in non-aqueous solution, Gel displays an amorphous halo with maximum at nearly 20.8° proving its amorphous structure [45].

The WAXS profiles of PCL/Gel blends and their CNF-loaded nanocomposites are depicted in Fig. 9 and compared with pure electrospun PCL. In addition, crystallinity of the samples was calculated using Eq. 1 which is given in Table 5. Firstly, it is visible that upon Gel blending, the PCL crystallinity was significantly reduced as seen by the absence of peak positioned at ca. 19.5° and dramatic intensity reduction in peaks at $2\theta = 21.3°$ and 23.6°. Comparing P70, P50, and P30, it is clarified that as more Gel was incorporated, the further reduction in crystallinity was occurred. This phenomenon could be attributed to the possible interactions, in the form of hydrogen bonding, among two polymers. It might be believed that such probable interactions interrupt the orientation order of PCL macromolecules chains.

The WAXS patterns of PCl/GeL/CNF (Fig. 9) confirm the presence of CNF in nanocomposites, so that after CNF addition, PCL crystalline peaks were

intensified which proves the crystallinity enhancement (Table 5). The reports imply that the impact of nanofiller incorporation on crystallinity of semicrystalline could be either destructive or constructive depending on filler content, its dispersion level, and/or its possible interactions with the polymer [49, 63]. A good dispersion could normally lead to heterogeneous nucleation, whereas likely interactions can suppress crystallinity. In current work, although hydrogen bonding interactions can be most probably took place between CNF and Gel, it seems that well CNF dispersion, due to high shear applied along the electrospinning, has overcome the devastating effect of such interactions, and consequently, the crystallinity was increased.

DSC analysis

Differential scanning calorimetry was employed to monitor thermal behavior of PCL, P70, and P70+ 2%CNF samples (Fig. 10). All the samples display a wide endothermic peak with an extremum positioned in the range of 60–70 °C. For each sample, the starting point of endothermic peak is the temperature in which PCL crystals begin to fuse, while the peak endpoint is where crystals are completely melted. The peak area was used to calculate the melting enthalpy (ΔH) of each sample. The measured enthalpy for PCL, P70, and P70+ 2%CNF were 58.4, 42.7, and 45.57 J/g, respectively. As the melting enthalpy is directly proportional to crystallinity [49], the results revealed that upon Gel blending, the PCL crystallinity decreased, while CNF addition increased the crystallinity. These results are in agreement with the crystallinity obtained from WAXS.
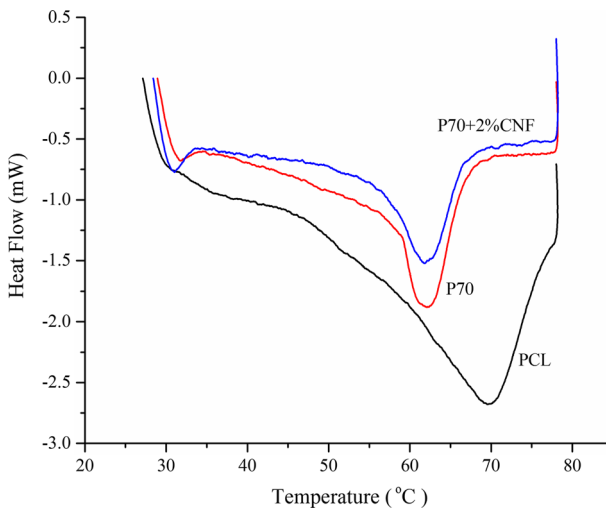

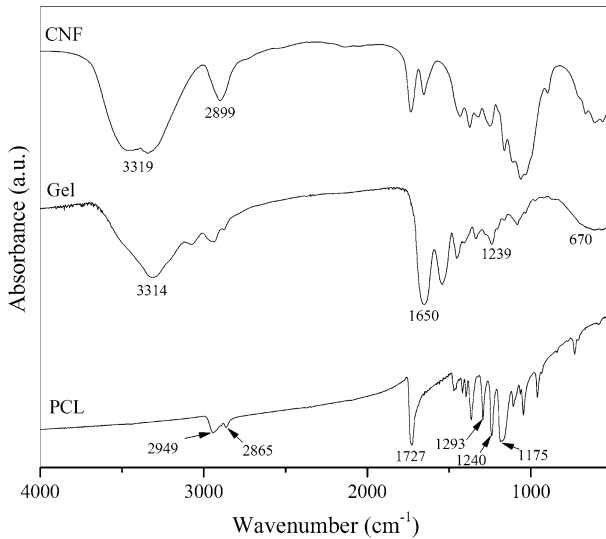**Fig. 10** DSC thermograms of electrospun samples

Fig. 11 CNF, Gel, and PCL FTIR spectra

FTIR spectra

It is widespread to use FTIR analysis as an evidence for proving the presence of polymers and nanomaterials in composites as well as their possible interaction. Therefore, the same procedure was carried out to chemically investigate the chemistry of spun fibrous nanocomposites. The FTIR spectrums of PCL, Gel, and CNF are depicted in Fig. 11; accordingly, their main absorption bands are listed in Table 6.

When PCL and Gel were blended and electrospun, some distinct changes were emerged in association with IR spectra when compared with pure polymers, which are visible in Fig. 12. According to this figure, mixing 30 wt% Gel and 70 wt% PCL (sample P70) caused the appearance of a weak peak at 3300 cm^{-1} assigned to amide N–H stretching which is stronger in the case of P30 (70 wt% of Gel). Furthermore, CH$_2$ stretching (positioned at 2949 cm^{-1}) peaks for PCL were shifted to nearly 2943 cm^{-1} and 2937 cm^{-1}, respectively, for P70 and P30. The similar trend was also observed for C=O stretching, particularly for P30, in which the band was shifted to 1723 cm^{-1}. Appearance of new peaks, as well as shifting and broadening of the peaks, could be the witnesses for presence of both polymers in the blend and probable interactions among them.

As a result of CNF addition to PCL/Gel blends, the changes were more interesting (Fig. 12). Firstly, it can be clearly seen that amide N–H stretching intensity at around 3300 cm^{-1} significantly weakened after CNF incorporation. Secondly, CNF reshaped the carbonyl peak (1650 cm^{-1}) from a sharper to a wider peak, which is more visible for the composite including 70 wt% Gel. It is deduced that due to the presence of carboxyl and amine groups in Gel and also hydroxyl and methylol groups in cellulose, the strong hydrogen bonds are most probably formed between the components, which in turn led to alteration in FTIR absorption peaks.

Table 6 FTIR band assignments for CNF and electrospun PCL and Gel [38, 42]

| CNF	Assignment	ES-PCL	Assignment	ES-Gel	Assignment
897	β-Glycosidic linkages of glucose ring	1157	C–O and C–C stretching	670	N–H out of plane wagging
1035	C–O stretching	1175	C–O–C symmetric stretching	1239	CN stretching
1204	C–O deformation band	1240	C–O–C asymmetric stretching	1543	N–H bending
1335	O–H in-plane bending	1293	C–O and C–C stretching	1650	C=O stretching
1316	CH$_2$ wagging	1727	C=O stretching	3314	Amide N–H stretching
1639	O–H bending of adsorbed water	2865	Symmetric and asymmetric CH2 stretching		
2899	Aliphatic saturated C–H stretching vibration	2949	Symmetric and asymmetric CH2 stretching		
3319	O–H stretching				
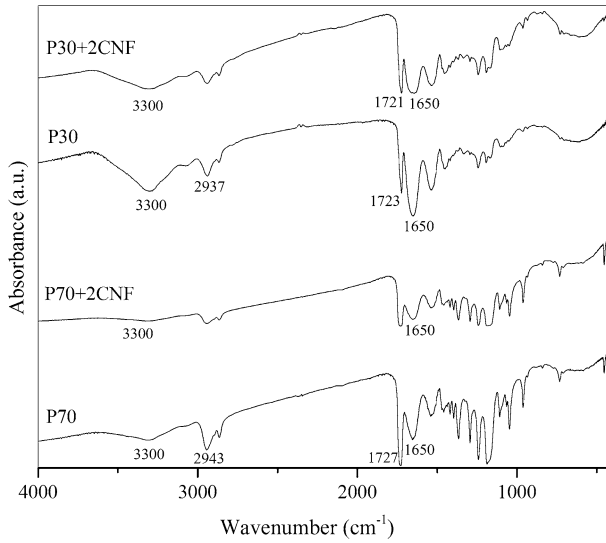
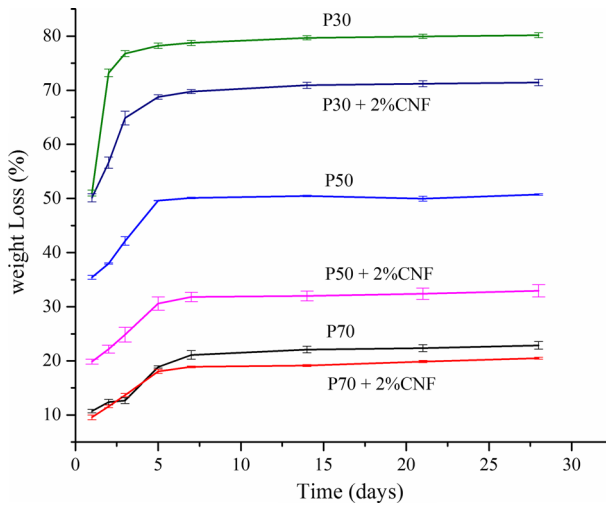**Fig. 12** PCL/Gel blends and PCL/Gel/CNF nanocomposites FTIR spectra

Fig. 13 In vitro degradability of electrospun nanocomposites in PBS solution

In vitro biodegradability

The changes in degradation rate of PCL/Gel and PCL/Gel/CNF (2 wt%) electrospun mats in 1, 2, 3, 5, 7, 14, 21, and 28 days are depicted in Fig. 13. Firstly, it can be seen that the highest weight loss occurs during 5-day incubation for all samples, and then it dramatically reduced. According to the literature [64], PCL degradation rate is smaller than Gel, which is due to semicrystalline nature of PCL, and

amorphous areas have significantly higher degradation. The rate of degradation of PCL/Gel proves this phenomenon, as Fig. 13 shows by increasing Gel content, the degradability increases, up to 80% loss weight for P30. Taking into account impact of CNF addition on degradability behavior of the PCL/Gel, it is observed that such nanofibers reduced degradation rate, which is statistically significant for P50 and P30. This event can be explained by changes in crystallinity of PCL/Gel in the presence of CNF. According to Table 5, CNF incorporation increased the crystallinity of PCL/Gel blends; hence, a reduction in degradation rate is anticipated. From a point of view, CNF acts as physical cross-linking agent which stabilizes PCL/Gel against biodegradation.

Conclusion

Novel fibrous nanocomposites of PCL/Gel/CNF were successfully electrospun for the first time. Morphological exploration via SEM showed a drastic reduction in fiber diameter upon 30 wt% Gel addition to PCL; however, more content of Gel led to increase in diameter, attributable to Gel emulsion. The addition of CNF to PCL/Gel blends also increased the mean fiber diameter. The electrospun nanocomposites were analyzed mechanically in tensile mode. It was confirmed that PCL and Gel, according to their intrinsic characteristics, resulted in softer and more brittle electrospun mats, respectively. In the case of CNF incorporation to the PCL/Gel blends, there was an optimum level of 2 wt% for UTS and Young's modulus, as in higher contents these parameters were reduced, mostly because of CNF agglomerations. The maximum UTS (3.24 ± 0.22) and Young's modulus (93.89 ± 10.44) belonged to P70/2CNF and P30/2CNF samples, respectively.

The existence of PCL, Gel, and CNF in nanocomposites was confirmed by FTIR and WAXS measurements. Both electrospinning and Gel blending ended to crystallinity reduction in PCL form 59.42% for granular PCL to 21. 92% for P30 sample. However, CNF addition caused increase in crystallinity of PCL/Gel blends. The DSC results also confirmed crystallinity changes are in agreement with WAXS. FTIR analysis proved possible interactions among the components which were confirmed by shift in peaks positions as well as their intensity reduction. The in vitro degradation of electrospun fibers in PBS solution was studied. Although increase in Gel content resulted in higher degradability of PCL/Gel blends, CNF incorporation enhanced the degradation resistance of the blends.

References

1. Rhim J-W, Ng PK (2007) Natural biopolymer-based nanocomposite films for packaging applications. Crit Rev Food Sci Nutr 47(4):411–433
2. Cha DS, Chinnan MS (2004) Biopolymer-based antimicrobial packaging: a review. Crit Rev Food Sci Nutr 44(4):223–237
3. Yang L, Hsiao W, Chen P (2002) Chitosan–cellulose composite membrane for affinity purification of biopolymers and immunoadsorption. J Membr Sci 197(1–2):185–197

4. Dashtimoghadam E, Hasani-Sadrabadi MM, Moaddel H (2010) Structural modification of chitosan biopolymer as a novel polyelectrolyte membrane for green power generation. Polym Adv Technol 21(10):726–734

5. Ghasemi-Mobarakeh L, Prabhakaran MP, Balasubramanian P, Jin G, Valipouri A, Ramakrishna S (2013) Advances in electrospun nanofibers for bone and cartilage regeneration. J Nanosci Nanotechnol 13(7):4656–4671

6. Stoppel WL, Ghezzi CE, McNamara SL, Black LD III, Kaplan DL (2015) Clinical applications of naturally derived biopolymer-based scaffolds for regenerative medicine. Ann Biomed Eng 43(3):657–680

7. Huang Z-M, Zhang Y, Ramakrishna S, Lim C (2004) Electrospinning and mechanical characterization of gelatin nanofibers. Polymer 45(15):5361–5368

8. Jayakumar R, Prabaharan M, Nair S, Tamura H (2010) Novel chitin and chitosan nanofibers in biomedical applications. Biotechnol Adv 28(1):142–150

9. Moon S, Ryu BY, Choi J, Jo B, Farris RJ (2009) The morphology and mechanical properties of sodium alginate based electrospun poly (ethylene oxide) nanofibers. Polym Eng Sci 49(1):52–59

10. Zhang Y, Venugopal J, Huang Z-M, Lim C, Ramakrishna S (2005) Characterization of the surface biocompatibility of the electrospun PCL-collagen nanofibers using fibroblasts. Biomacromol 6(5):2583–2589

11. Li Z-F, Zhang H, Liu Q, Sun L, Stanciu L, Xie J (2013) Fabrication of high-surface-area graphene/polyaniline nanocomposites and their application in supercapacitors. ACS Appl Mater Interfaces 5(7):2685–2691

12. Neisiany RE, Khorasani SN, Kong Yoong Lee J, Ramakrishna S (2016) Encapsulation of epoxy and amine curing agent in PAN nanofibers by coaxial electrospinning for self-healing purposes. RSC Adv 6(74):70056–70063. https://doi.org/10.1039/C6RA06434E

13. Arrieta MP, López J, López D, Kenny J, Peponi L (2016) Biodegradable electrospun bionanocomposite fibers based on plasticized PLA–PHB blends reinforced with cellulose nanocrystals. Ind Crops Prod 93:290–301

14. Cai N, Dai Q, Wang Z, Luo X, Xue Y, Yu F (2015) Toughening of electrospun poly (L-lactic acid) nanofiber scaffolds with unidirectionally aligned halloysite nanotubes. J Mater Sci 50(3):1435–1445

15. Woodruff MA, Hutmacher DW (2010) The return of a forgotten polymer—polycaprolactone in the 21st century. Prog Polym Sci 35(10):1217–1256

16. Fang R, Zhang E, Xu L, Wei S (2010) Electrospun PCL/PLA/HA based nanofibers as scaffold for osteoblast-like cells. J Nanosci Nanotechnol 10(11):7747–7751

17. Nitya G, Nair GT, Mony U, Chennazhi KP, Nair SV (2012) In vitro evaluation of electrospun PCL/nanoclay composite scaffold for bone tissue engineering. J Mater Sci Mater Med 23(7):1749–1761

18. Augustine R, Malik HN, Singhal DK, Mukherjee A, Malakar D, Kalarikkal N, Thomas S (2014) Electrospun polycaprolactone/ZnO nanocomposite membranes as biomaterials with antibacterial and cell adhesion properties. J Polym Res 21(3):347

19. Gaharwar AK, Mukundan S, Karaca E, Dolatshahi-Pirouz A, Patel A, Rangarajan K, Mihaila SM, Iviglia G, Zhang H, Khademhosseini A (2014) Nanoclay-enriched poly (ε-caprolactone) electrospun scaffolds for osteogenic differentiation of human mesenchymal stem cells. Tissue Eng Part A 20(15–16):2088–2101

20. Scaffaro R, Lopresti F, Maio A, Botta L, Rigogliuso S, Ghersi G (2017) Electrospun PCL/GO-g-PEG structures: processing-morphology-properties relationships. Compos A Appl Sci Manuf 92:97–107

21. Espadín A, De Dios LT, Ruvalcaba E, Valadez-García J, Velasquillo C, Bustos-Jaimes I, Vázquez-Torres H, Gimeno M, Shirai K (2018) Production and characterization of a nanocomposite of highly crystalline nanowhiskers from biologically extracted chitin in enzymatic poly (ε-caprolactone). Carbohyd Polym 181:684–692

22. Naghieh S, Foroozmehr E, Badrossamay M, Kharaziha M (2017) Combinational processing of 3D printing and electrospinning of hierarchical poly (lactic acid)/gelatin-forsterite scaffolds as a biocomposite: mechanical and biological assessment. Mater Des 133:128–135

23. Kharaziha M, Fathi M, Edris H (2013) Tunable cellular interactions and physical properties of nanofibrous PCL-forsterite: gelatin scaffold through sequential electrospinning. Compos Sci Technol 87:182–188

24. Loh QL, Choong C (2013) Three-dimensional scaffolds for tissue engineering applications: role of porosity and pore size. Tissue Eng B: Rev 19(6):485–502

25. Dórame-Miranda RF, Rodríguez-Félix DE, López-Ahumada GA, Castro-Enriquez DD, Quiroz-Castillo JM, Márquez-Ríos E, Rodríguez-Félix F (2018) Effect of pH and temperature on the release kinetics of urea from wheat-gluten membranes obtained by electrospinning. Polym Bull 75(11):5305–5319. https://doi.org/10.1007/s00289-018-2327-9

26. Sangeetha K, Alsharani FA, Angelin Vinodhini P, Sudha PN, Jayachandran V, Sukumaran A (2018) Antimicrobial efficacy of novel nanochitosan-based mat via electrospinning technique. Polym Bull 75(12):5599–5618. https://doi.org/10.1007/s00289-018-2324-z

27. Neisiany RE, Khorasani SN, Naeimirad M, Lee JKY, Ramakrishna S (2017) Improving mechanical properties of carbon/epoxy composite by incorporating functionalized electrospun polyacrylonitrile nanofibers. Macromol Mater Eng 302(5):1600551. https://doi.org/10.1002/mame.201600551

28. Liu X, Ma PX (2009) Phase separation, pore structure, and properties of nanofibrous gelatin scaffolds. Biomaterials 30(25):4094–4103

29. Akbarzadeh R, Yousefi AM (2014) Effects of processing parameters in thermally induced phase separation technique on porous architecture of scaffolds for bone tissue engineering. J Biomed Mater Res B Appl Biomater 102(6):1304–1315

30. Hou Q, Grijpma DW, Feijen J (2003) Preparation of interconnected highly porous polymeric structures by a replication and freeze-drying process. J Biomed Mater Res B Appl Biomater 67(2):732–740

31. Baker SC, Rohman G, Southgate J, Cameron NR (2009) The relationship between the mechanical properties and cell behaviour on PLGA and PCL scaffolds for bladder tissue engineering. Biomaterials 30(7):1321–1328

32. Famili M, Janani H, Enayati M (2011) Foaming of a polymer–nanoparticle system: effect of the particle properties. J Appl Polym Sci 119(5):2847–2856

33. Enayati M, Famili MHN, Janani H (2013) Open-celled microcellular foaming and the formation of cellular structure by a theoretical pattern in polystyrene. Iran Polym J 22(6):417–428

34. Enayati M, Famili M, Janani H (2010) Production of polystyrene open-celled microcellular foam in batch process by super critical CO_2. Iran J Polym Sci Technol 23:223–234 **(In Persian)**

35. Neisiany RE, Khorasani SN, Lee JKY, Naeimirad M, Ramakrishna S (2018) Interfacial toughening of carbon/epoxy composite by incorporating styrene acrylonitrile nanofibers. Theor Appl Fract Mech 95:242–247

36. Razavi S, Neisiany RE, Ayatollahi M, Ramakrishna S, Khorasani SN, Berto F (2018) Fracture assessment of polyacrylonitrile nanofiber-reinforced epoxy adhesive. Theor Appl Fract Mech 97:448–453

37. Razavi SMJ, Neisiany RE, Khorasani SN, Ramakrishna S, Berto F (2018) Effect of neat and reinforced polyacrylonitrile nanofibers incorporation on interlaminar fracture toughness of carbon/epoxy composite. Theor Appl Mech Lett 8(2):126–131

38. Ghasemi-Mobarakeh L, Prabhakaran MP, Morshed M, Nasr-Esfahani M-H, Ramakrishna S (2008) Electrospun poly (ε-caprolactone)/gelatin nanofibrous scaffolds for nerve tissue engineering. Biomaterials 29(34):4532–4539

39. Ji W, Yang F, Ma J, Bouma MJ, Boerman OC, Chen Z, van den Beucken JJ, Jansen JA (2013) Incorporation of stromal cell-derived factor-1α in PCL/gelatin electrospun membranes for guided bone regeneration. Biomaterials 34(3):735–745

40. Chen Z, Cao L, Wang L, Zhu H, Jiang H (2013) Effect of fiber structure on the properties of the electrospun hybrid membranes composed of poly (ε-caprolactone) and gelatin. J Appl Polym Sci 127(6):4225–4232

41. Xue J, He M, Liang Y, Crawford A, Coates P, Chen D, Shi R, Zhang L (2014) Fabrication and evaluation of electrospun PCL–gelatin micro-/nanofiber membranes for anti-infective GTR implants. J Mater Chem B 2(39):6867–6877

42. Ren K, Wang Y, Sun T, Yue W, Zhang H (2017) Electrospun PCL/gelatin composite nanofiber structures for effective guided bone regeneration membranes. Mater Sci Eng C 78:324–332

43. Saadatkish N, Nouri Khorasani S, Morshed M, Allafchian A-R, Beigi M-H, Masoudi Rad M, Esmaeely Neisiany R, Nasr-Esfahani M-H (2018) A ternary nanofibrous scaffold potential for central nerve system tissue engineering. J Biomed Mater Res, Part A 106(9):2394–2401. https://doi.org/10.1002/jbm.a.36431

44. Zhang Y, Ouyang H, Lim CT, Ramakrishna S, Huang ZM (2005) Electrospinning of gelatin fibers and gelatin/PCL composite fibrous scaffolds. J Biomed Mater Res B Appl Biomater 72(1):156–165

45. Denis P, Dulnik J, Sajkiewicz P (2015) Electrospinning and structure of bicomponent polycaprolactone/gelatin nanofibers obtained using alternative solvent system. Int J Polym Mater Polym Biomater 64(7):354–364

46. Gautam S, Dinda AK, Mishra NC (2013) Fabrication and characterization of PCL/gelatin composite nanofibrous scaffold for tissue engineering applications by electrospinning method. Mater Sci Eng C 33(3):1228–1235

47. Rajzer I, Menaszek E, Kwiatkowski R, Planell JA, Castano O (2014) Electrospun gelatin/poly (ε-caprolactone) fibrous scaffold modified with calcium phosphate for bone tissue engineering. Mater Sci Eng C 44:183–190

48. Lee J, Deng Y (2013) Nanoindentation study of individual cellulose nanowhisker-reinforced PVA electrospun fiber. Polym Bull 70(4):1205–1219

49. Enayati MS, Behzad T, Sajkiewicz P, Bagheri R, Ghasemi-Mobarakeh L, Kuśnieruk S, Rogowska-Tylman J, Pahlevanneshan Z, Choińska E, Święszkowski W (2016) Fabrication and characterization of electrospun bionanocomposites of poly (vinyl alcohol)/nanohydroxyapatite/cellulose nanofibers. Int J Polym Mater Polym Biomater 65(13):660–674

50. Enayati MS, Neisiany RE, Sajkiewicz P, Behzad T, Denis P, Pierini F (2019) Effect of nanofiller incorporation on thermomechanical and toughness of poly (vinyl alcohol)-based electrospun nanofibrous bionanocomposites. Theor Appl Fract Mech 99:44–50. https://doi.org/10.1016/j.tafmec.2018.11.006

51. Peresin MS, Habibi Y, Zoppe JO, Pawlak JJ, Rojas OJ (2010) Nanofiber composites of polyvinyl alcohol and cellulose nanocrystals: manufacture and characterization. Biomacromol 11(3):674–681

52. Bellani CF, Pollet E, Hebraud A, Pereira FV, Schlatter G, Avérous L, Bretas RE, Branciforti MC (2016) Morphological, thermal, and mechanical properties of poly (ε-caprolactone)/poly (ε-caprolactone)-grafted-cellulose nanocrystals mats produced by electrospinning. J Appl Polym Sci 133 (21):43445. https://doi.org/10.1002/app.43445

53. Rezvani Ghomi E, Khalili S, Nouri Khorasani S, Esmaeely Neisiany R, Ramakrishna S (2019) Wound dressings: Current advances and future directions. J Appl Polym Sci 136 (27):47738. doi:10.1002/app.47738

54. Enayati MS, Behzad T, Sajkiewicz P, Rafienia M, Bagheri R, Ghasemi-Mobarakeh L, Kolbuk D, Pahlevanneshan Z, Bonakdar SH (2018) Development of electrospun poly (vinyl alcohol)-based bionanocomposite scaffolds for bone tissue engineering. J Biomed Mater Res Part A 106(4):1111–1120

55. Zoppe JO, Peresin MS, Habibi Y, Venditti RA, Rojas OJ (2009) Reinforcing poly(ε-caprolactone) nanofibers with cellulose nanocrystals. Appl Mater Interf 1:1996–2004

56. Vatankhah E, Prabhakaran MP, Jin G, Mobarakeh LG, Ramakrishna S (2014) Development of nanofibrous cellulose acetate/gelatin skin substitutes for variety wound treatment applications. J Biomater Appl 28(6):909–921

57. Khalili S, Khorasani SN, Neisiany RE, Ramakrishna S (2019) Theoretical cross-link density of the nanofibrous scaffolds. Mat Design Process Comm 1(1):e22. https://doi.org/10.1002/mdp2.22

58. Mark JE (2007) Physical properties of polymers handbook, vol 1076. Springer, Berlin

59. Enayati MS, Behzad T, Sajkiewicz P, Bagheri R, Ghasemi-Mobarakeh L, Pierini F (2018) Theoretical and experimental study of the stiffness of electrospun composites of poly (vinyl alcohol), cellulose nanofibers, and nanohydroxy apatite. Cellulose 25(1):65–75

60. Vatankhah E, Semnani D, Prabhakaran MP, Tadayon M, Razavi S, Ramakrishna S (2014) Artificial neural network for modeling the elastic modulus of electrospun polycaprolactone/gelatin scaffolds. Acta Biomater 10(2):709–721

61. Rajzer I, Menaszek E, Kwiatkowski R, Chrzanowski W (2014) Bioactive nanocomposite PLDL/nano-hydroxyapatite electrospun membranes for bone tissue engineering. J Mater Sci Mater Med 25(5):1239–1247. https://doi.org/10.1007/s10856-014-5149-9

62. Koosha M, Mirzadeh H, Shokrgozar MA, Farokhi M (2015) Nanoclay-reinforced electrospun chitosan/PVA nanocomposite nanofibers for biomedical applications. RSC Adv 5(14):10479–10487

63. Enayati MS, Behzad T, Sajkiewicz P, Bagheri R, Ghasemi-Mobarakeh L, Łojkowski W, Pahlevanneshan Z, Ahmadi M (2016) Crystallinity study of electrospun poly (vinyl alcohol) nanofibers: effect of electrospinning, filler incorporation, and heat treatment. Iran Polym J 25(7):647–659

64. Cohn D, Salomon AH (2005) Designing biodegradable multiblock PCL/PLA thermoplastic elastomers. Biomaterials 26(15):2297–2305

Affiliations

Zahra Moazzami Goudarzi[1] · Tayebeh Behzad[1] · Laleh Ghasemi-Mobarakeh[2] · Mahshid Kharaziha[3] · Mohammad Saied Enayati[1,4]

[1] Department of Chemical Engineering, Isfahan University of Technology, Isfahan 84156-83111, Iran

[2] Department of Textile Engineering, Isfahan University of Technology, Isfahan 84156-83111, Iran

[3] Department of Materials Engineering, Isfahan University of Technology, Isfahan 84156-83111, Iran

[4] Institute of Fundamental Technological Research, Polish Academy of Sciences, Pawinskiego 5B, 02-106 Warsaw, Poland